

ELECTROMAGNETIC EMBEDDING

A. M. van de Water, B. P. de Hon, A. G. Tijhuis, M. C. van Beurden
Faculty of Electrical Engineering, Eindhoven University of Technology,
P.O. Box 513, 5600 MB Eindhoven, The Netherlands.

Abstract: Linear embedding via Green's operators (LEGO) is a diakoptic modeling procedure based on equivalence principles for the electromagnetic characterization of finite composite structures of arbitrary shape through equivalent currents on their boundary, as if they were multi-port systems. To avoid spurious resonances that may appear when using Schelkunoff's equivalence principle, we have extended LEGO to the 3-D case in the framework of Love's equivalence principle, involving both electric and magnetic current sources. Multiple scattering between adjacent domains is accounted for by considering one domain as the environment of the other and vice versa, resulting in one new composite scattering domain.

INTRODUCTION

In its present form, the idea of embedding arose in inverse scattering [1] from a reluctance to perform de-embedding, which, like deconvolution, is not stable *per se*. Linear embedding via Green's operators (LEGO) may be regarded as a specific Green's function variety of Krohn's diakoptics [2], set in the mathematical framework of the equivalence principles of Love and/or Schelkunoff. The equivalent surface-source distributions are not unique, e.g., Love's equivalence principle (LEP) involves a combination of electric and magnetic current sources, and produces a null field in the environment, whereas Schelkunoff's equivalence principle (SEP) states that it suffices to consider either electric, or magnetic equivalent current surface sources.

LEGO may be used to describe multiple scattering between adjacent objects, by considering one of the objects as the environment of the other and vice versa. Our implementation relies on an operator formalism [3, 4], involving source-to-source scattering and reflection operators that account for the respective scattering from an object and its environment. Thus, formal manipulations are kept simple enough to allow for any cascade of embedding steps, by which the electromagnetic response of large, intricate, possibly resonant structures is readily obtained from the electromagnetic response of elementary building blocks.

In previous work, we have generalized the embedding technique to account for the multiple scattering between two disjoint computational domains of general shape containing different objects [5]. We validated it with a boundary integral equation (BIE) for multiple dielectric objects [6], and demonstrated the wide applicability as a design tool in the field of (finite) electromagnetic bandgap (EBG) structures [7]. In [3], we have shown that the embedding procedure based on SEP suffers from spurious interior resonance modes when common boundary parts are removed, and implemented LEP to avoid this drawback. Up to now, we have presented the embedding technique for two-dimensional (2D) configurations only. Below, we explain the embedding technique in a generic form, and present the first implementation in a full three-dimensional (3D) configuration based on LEP.

EMBEDDING CONCEPT

To illustrate the embedding concept, we consider the scattering problem depicted in Fig. 1, involving two scattering domains, \mathcal{D}_1 and \mathcal{D}_2 , bounded by the surfaces \mathcal{S}_1 and \mathcal{S}_2 , respectively. The observation surfaces, as well as the scattering objects inside the domains may be of arbitrary shape. The embedding technique accounts for the electromagnetic interaction between both domains. It provides the multiple scattering in terms of the scattering operators of the individual domains that have been characterized at an earlier stage. The scattering operator of a domain, say \mathcal{D}_1 , denoted by \mathcal{S}_{11} , constitutes a mapping from the equivalent current source distributions J^{in} associated with an arbitrary incident field on \mathcal{D}_1 , to equivalent current distributions J^{sc} , associated with the corresponding scattered field exterior to \mathcal{D}_1 . Both J^{in} and J^{sc} may contain electric, as well as magnetic equivalent current components, depending on the applied equivalence principle.

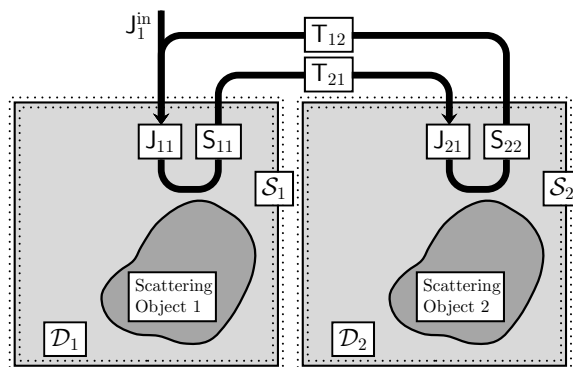


Figure 1: The J_{11} and J_{21} operators for an incident current J_1^{in} on S_1 that include the direct incident field and the occurring multiple scattering represented by the loop.

In order to obtain the complete field, i.e., the total field in the combined configuration, we would have to replace the incident current distributions J^{in} , associated with the single scattering domains, with equivalent 'complete' current distributions J^{cp} that include the multiple scattering contributions. To accomplish this, we introduce four J operators,

$$\begin{bmatrix} J_1^{\text{cp}} \\ J_2^{\text{cp}} \end{bmatrix} = \begin{bmatrix} J_{11} & J_{12} \\ J_{21} & J_{22} \end{bmatrix} \begin{bmatrix} J_1^{\text{in}} \\ J_2^{\text{in}} \end{bmatrix}. \quad (1)$$

From left to right, the subscripts of the J operator elements respectively denote the surfaces on which the observation and source distributions are located. For example, J_{12} yields an equivalent current distribution on S_1 for the complete field in \mathcal{D}_1 due to the field incident on \mathcal{D}_2 . Once the four J operators have been determined, the entire field problem has effectively been solved, and a new scattering operator of the combined structure can be formed by application of the scattering operators of the individual domains.

The J operators are obtained by considering domain \mathcal{D}_2 as part of the environment of \mathcal{D}_1 and vice versa. In this approach, the exterior and interior fields of the individual domains are related through two current-transfer operators, T_{21} and T_{12} . The action of the transfer operators is depicted in Fig. 1. Here, the T_{21} operator produces an equivalent current distribution on S_2 for the field in \mathcal{D}_2 associated with a current source distribution on S_1 . The part of the multiple scattering process that is relevant for the construction of J_{11} and J_{21} involves the incident field on S_1 only. A similar loop can be constructed for J_{12} and J_{22} . Hence, once the scattering operators of both domains are connected through transfer operators, thereby creating the closed loop in Fig. 1, the multiple scattering phenomenon is tackled, and a new scattering operator of the combined structure can be composed by application of the individual scattering operators.

EMBEDDING OF 3D OBJECTS

The embedding technique accounts for objects of arbitrary shape. Here, we consider the two homogeneous dielectric spheres depicted in Fig. 2., with radius a and permittivity $\epsilon_r = 20$, for $k_0 a = 1.5$, as a first proof of principle of embedding applied to 3D structures. With the embedding technique, the scattering operator of the combination of spheres is composed from the scattering operators of the individual spheres. Because closed structures are prone to spurious interior resonance modes, LEP is used.

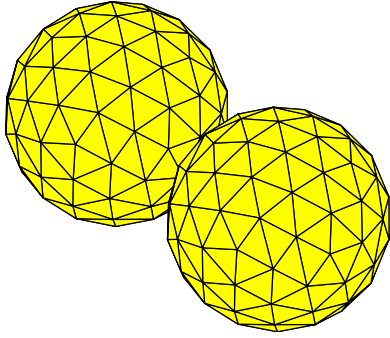


Figure 2: Two dielectric spheres with radius a at $k_0 a = 1.5$ with $\epsilon_r = 20$ that are separated by $0.2a$. Each sphere is meshed with 192 triangles (288 unknowns).

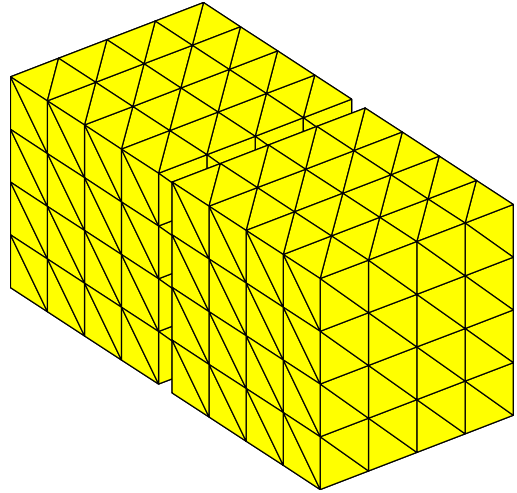


Figure 3: Two cubical domains that enclose the two spheres in Fig. 2. The cubes are meshed with 192 triangles (288 unknowns) with an edge length of $2.2a$.

First, we construct the scattering operator of a single sphere inside a cubical scattering domain, see Fig. 3, with edge length $2.2a$. In our approach, we expand all current distributions in terms of Rao, Wilton, and Glisson (RWG) basis functions, denoted by f_n . The scattering of a sphere in a homogeneous background is obtained via the commonly used *Poggio, Miller, Chang, Harrington, Wu* (PMCHW) BIE formulation [8]. In our case, the incident fields to be considered in the PMCHW formulation, are the fields incident on the sphere due to each RWG of the (expanded) incident current J^{in} . Once the PMCHW BIE has been solved via an iterative technique or, in the present case, an LU-decomposition, the resulting current distribution on the sphere is propagated (back) to the surface of the cubical scattering domain. On the boundary of the scattering domain we consider the field in a weak sense, i.e., we test the field with f_m and/or $n \times f_m$. By taking the exterior product with the unit normal on the surface and including an additional minus sign, a weighted form of the desired equivalent current distributions J^{sc} are obtained that would reproduce the pertaining exterior scattered fields. To retrieve the current amplitudes I_n^{sc} of f_n in J^{sc} , we apply the inverse Gramm matrix (see also [3] for the 2D case), where the Gramm operator represents the inner products of the test and expansion functions. The mapping of the current amplitudes I_n^{in} of the incident field to the current amplitudes I_n^{sc} of the scattered field forms the scattering operator. Note that the Gramm matrix must also be applied to the incident field to obtain the (initial) current amplitudes I_n^{in} . The integrals of the test- and expansion function are computed via adaptive Gaussian quadrature rules. In Fig. 4, the bistatic radar cross-section (RCS) of a single sphere is shown for both E and H polarization. As a comparison, the exact solution via the *Mie series* is shown. The deterioration in the RCS by considering the scattering operator on the surface of the cube instead of the direct PMCHW approach on the surface of the sphere appears to be negligible.

Second, the obtained scattering operator of a single sphere is combined with the same operator (for the second sphere) in the embedding procedure to arrive at the scattering operator of the two spheres. The second sphere is a translated version of the first. Apart from the scattering operator, the transfer operators T_{12} and T_{21} are also required to close the multiple scattering loop shown in Fig. 1. As for the composition of the scattering operator, all current source amplitudes on a cube are propagated to the adjacent cube, where the exterior product with the surface normal together with an additional minus sign is evaluated to obtain the equivalent current distribution that reproduces the incident field inside. Subsequent testing and application of the inverse Gramm operator completes the construction of the desired transfer operators that describe the electromagnetic communication between both domains. All operators required in the embedding procedure described above have now been discussed. In Fig. 5, the RCS of the two spheres is shown. The plane wave is incident from above with the E -plane aligned with the translation direction of the spheres. The result of the PMCHW formulation are included as a reference. The results agree very well with the results from the (combined) scattering

operator obtained from the embedding procedure. This is remarkable regarding the coarseness of the applied discretization. Note that the minute deviations may also be partially attributed to the PMCHW formulation.

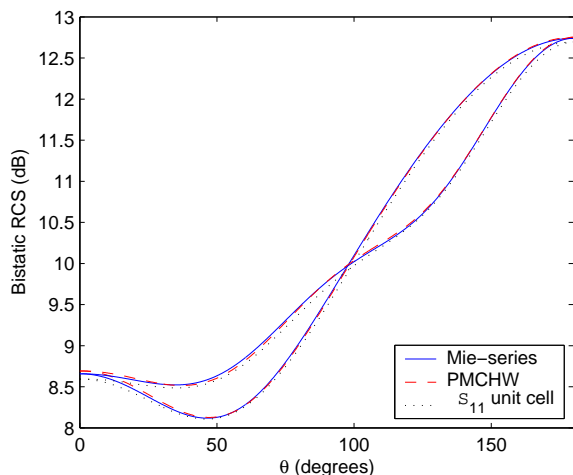


Figure 4: The bistatic RCS of one sphere of Fig. 2. The solid (blue) line is the Mie-series, the dashed (red) line the PMCHW BIE, and the dotted (black) line the S -operator of the same sphere inside one cube of Fig. 3.

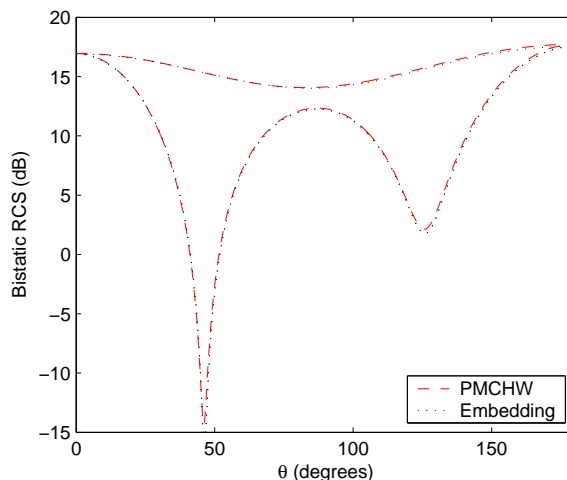


Figure 5: The bistatic RCS of the two dielectric spheres in Fig. 2. The dashed line (red) is the PMCHW BIE, and the dotted (black) line the embedding of the unit cells in Fig. 3 that enclose the same (discretized) spheres.

CONCLUSIONS

We have applied linear embedding via Green's operators (LEGO) to a full 3D configuration in the framework of Love's equivalence principle. The results for the embedding of two closely packed dielectric spheres are very accurate with respect to the BIE solution for multiple dielectric objects.

ACKNOWLEDGEMENTS

The research presented above has been financially supported by the Inter-University Research Institute COBRA, under Project No. 99004670.

REFERENCES

- [1] A. Franchois and A.G. Tijhuis, "A quasi-Newton reconstruction algorithm for a complex microwave imaging scanner environment", *Radio Science*, 38(2), 8011, 2003.
- [2] G. Krohn, "A Set of principles to interconnect the solutions of physical systems", *Journal of Applied Physics*, 2, 965, 1953.
- [3] A. M. van de Water, B. P. de Hon, M. C. van Beurden and A. G. Tijhuis, "Green's function diakoptics through embedding – General theory and numerical Aspects," *2003 ICEAA International Conference on Electromagnetics in Advanced Applications, Torino, Italy, 12–16 Sept.*
- [4] A. M. van de Water, B. P. de Hon, M. C. van Beurden and A. G. Tijhuis, "Linear embedding via Green's operators—A modeling technique for finite electromagnetic bandgap structures", *Submitted to Physical Review E*
- [5] A. G. Tijhuis, M. C. van Beurden, and E. Korkmaz, "Modeling electromagnetic fields in large, finite structures using iterative techniques and the equivalence principle", *2003 ICEAA International Conference on Electromagnetics in Advanced Applications, Torino, Italy, 8–12 Sept.*
- [6] A. M. van de Water, B. P. de Hon, M. C. van Beurden, A. G. Tijhuis, and P. de Maagt, "Electromagnetic modelling of composite finite structures by embedding", *2004 URSI International Symposium on Electromagnetic Theory, Pisa, Italy, 23–27 May.*
- [7] A. M. van de Water, B. P. de Hon, M. C. van Beurden, A. G. Tijhuis, and P. de Maagt, "An embedding approach for electromagnetic field modeling in finite EBG Structures", *2004 27th ESA Antenna Technology Workshop on Innovative Periodic Antennas, Santiago de Compostella, Spain, 8–11 March.*
- [8] K. Umashankar, A. Taflove, and S. M. Rao, "Electromagnetic scattering by arbitrary shaped three-dimensional homogeneous lossy dielectric objects", *Trans. Antennas Propagat.*, 34(6), 758–66, 1986.